Cluster Orbital Theory Based on Mössbauer Effect Investigations of the (Iron)$_4$-Sulfur Clusters of *Clostridium pasteurianum* Ferredoxin

Hermann Eicher, Fritz Parak, Ludwig Bogner
Physik Department der Technischen Universität München

and

Klaus Gersonde
Abteilung Physiologische Chemie der Rheinisch-Westfälischen Technischen Hochschule Aachen

(Z. Naturforsch. **29 c**, 683–691 [1974] ; received September 2, 1974)

Mössbauer Effect, Cluster Orbital Theory, Ferredoxin, *Clostridium pasteurianum*

A cluster orbital theory is developed, which allows the calculation of Mössbauer spectra of oxidized and reduced ferredoxin of *Clostridium pasteurianum* under the conditions of low temperature (4.2 K) and high external magnetic field ($\boldsymbol{H}_{ex} \gtrsim 1$ T). The calculations are based on the symmetry properties of the problem and the way in which these symmetries are reflected in the (iron)$_4$-sulfur cluster wave function. The assumed cubic T_d symmetry of the cluster implies an isotropic interaction with the applied external magnetic field, where the average g-tensor is taken to be $g=1.944$ in accordance with ESR results. The magnetic hyperfine interaction of the cluster electrons with the magnetic dipole moments of the iron nuclei is defined by two parameters $\varkappa$ and ϱ reflecting trigonal point symmetry C_{3v} of each iron site. These parameters are determined by a least squares fit of the experimental Mössbauer spectrum of reduced ferredoxin at 4.2 K and $\boldsymbol{H}_{ext}=2$ T. In correspondence with the theory, $\varkappa$ and ϱ have been proved to be independent of $\boldsymbol{H}_{ext}$. Despite neglecting small deviations from T_d and C_{3v} point symmetry of the center of the cluster and the iron sites, respectively, theory and experiments are in reasonable good agreement.

Introduction

Recently we have published experimental results of Mössbauer and ESR investigations of *Clostridium pasteurianum* ferredoxin. On this basis a qualitative physical model of a two-cluster ferredoxin was proposed which explains the unexpected magnetic behaviour of oxidized ferredoxin (Fd_{ox}) and of reduced ferredoxin (Fd_{red})[1,2]. Fd_{ox} exhibits no paramagnetic resonance at 4.2 K. From the low temperature Mössbauer spectrum of Fd_{ox} it was concluded that the high spin iron(III) atoms in each (iron)$_4$-sulfur cluster are coupled to result in a spin $S=0$. Line broadening and the appearance of at least two partly resolved quadrupole doublets indicate that the iron atoms are not exactly equivalent with regard to their local symmetry. On reduction each cluster takes up one electron giving rise to an effective spin $S=1/2$. Spin-spin coupling of the two clusters removes the degeneracy of the total spin $S=1$ and prevents the appearance of a magnetic hyperfine splitting at 4.2 K. This mechanism is also responsible for the ESR signals as obtained in a magnetic field of 0.35 T. The effect of this small cluster-cluster coupling is cancelled out by the Zeeman interaction of an applied magnetic field $\boldsymbol{H}_{ext} \gtrsim 1$ T. In this case the spectral features of clusters with an effective spin $S=1/2$ are observed.

At the same time Mössbauer experiments on *Clostridium pasteurianum* ferredoxin were performed by Thompson *et al.*[3]. The results of these authors are in good agreement with the data published by us[1,2]. The interpretation of the Mössbauer spectra, however, has been based on different assumptions.

Thompson *et al.*[3] discuss the experimental spectra with respect to two models of the (iron)$_4$-sulfur clusters. On the one hand they assume four Fe(III) atoms antiferromagnetically coupled in Fd_{ox} to yield a non-magnetic state; on the other hand they propose two Fe(III) and two Fe(II) atoms antiferromagnetically coupled, this would also yield a non-magnetic oxidized state. On reduction one electron is accepted from each cluster, so that one Fe(III) atom changes to Fe(II) yielding $S=1/2$ for Fd_{red}. The authors of reference[3] emphasize that the observed quadrupole splittings and chemical shifts of Fd_{ox} are significantly greater than those

Requests for reprints should be sent to Dr. H. Eicher, Physik-Department, Technische Universität München, *D-8046 Garching bei München.*

expected for Fe(III) atoms and that no experimental evidence is given for separate Fe(III) and Fe(II) spectra of Fd_{ox} and in the high temperature spectra of Fd_{red}.

From the absence of separate Mössbauer patterns for Fe(III) and Fe(II) atoms it was concluded in reference [1, 2] that the transferred electrons should not be attributed to any particular iron site. The behaviour of the four iron atoms of the cluster has to be described by a wave function common to the outer electrons of all cluster atoms. This cluster orbital wave function has a non-magnetic singlet state for Fd_{ox} and a magnetic Kramers doublet for Fd_{red}. It is the purpose of this paper to develope this theoretical approach in detail and to apply it to the experimental results, especially to our published spectra of Fd_{red} obtained at 4.2 K in an external field of 2 T. The calculations are based on the symmetry properties of the cluster orbital wave function and its invariance under time reversal.

In its present state the theory does not treat cases which are characterized by a cluster-cluster interaction comparable to the Zeeman interaction of the applied magnetic field (*i. e.* cases of rather weak external fields). In agreement with ESR measurements we further assume that spin-lattice relaxation processes do not contribute significantly to the Mössbauer spectrum at 4.2 K in an external field.

The Hamiltonian

The steric arrangement of the atoms in one $(iron)_4$-sulfur cluster is shown in Fig. 1. The structure is based on the X-ray analysis of oxidized ferredoxin from *Peptococcus aerogenes* [4, 5] which is assumed to be closely related to the ferredoxin from *Clostridium pasteurianum* under investigation here. The four iron and the four so-called acid-labile sulfur atoms alternately occupy the corners of a cube. Actually the cube is not perfect but slightly distorted. In addition each iron atom is co-ordinated along the diagonal of the cube to a sulfur atom of a cysteine residue of the protein moiety. In a first approximation, the centre of a cluster has the point symmetry T_d and the four iron atoms have nearly trigonal point symmetry. In this approximation the four iron sites are assumed to be equivalent and the distortion of the cube has been neglected.

The energy levels of the cluster electrons are almost entirely determined by Coulomb and spin-orbit interactions. The interaction with an external magnetic field and the hyperfine interaction are considerably smaller and may be treated as perturbations. The corresponding Hamiltonian of these two perturbations is given by *

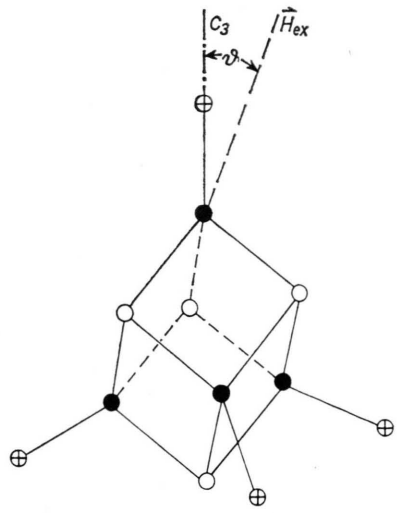

Fig. 1. Atomic model of the $(iron)_4$-sulfur cluster. Full circles represent iron atoms, open circles sulfur atoms, and crossed circles sulfur atoms of the cysteine residue.

$$\mathcal{H} = \beta_0 \boldsymbol{H}_{ext}\ g \boldsymbol{S}_{eff} + \beta_N g_I \sum_q (-1)^q \mathcal{T}_q^{(1)} \mathcal{K}_{-q}^{(1)} + P_{zz}[3\mathcal{I}_z^2 - I(I+1)] - \beta_N g_I \boldsymbol{H}_{ext} \boldsymbol{I}. \quad (1)$$

The first term represents the Zeeman interaction of the cluster electrons with an external magnetic field $\boldsymbol{H}_{ext}$, the second term describes the magnetic dipole hyperfine interaction and the third term the electric quadrupole hyperfine interaction between the cluster electrons and the appropriate nuclear moments; the last term relates to the direct Zeeman coupling of $\boldsymbol{H}_{ext}$ with the nuclear magnetic dipole moments. $\beta_0 = 0.4669$ (cm^{-1}/T) and $\beta_N = 2.542 \cdot 10^{-4}$ (cm^{-1}/T) are the Bohr and nuclear magneton, where the unit of magnetic field is Tesla (1 Tesla = 10 kG). Throughout the remainder of the paper the hyperfine energies are expressed in mm/s, the Doppler velocity between source and absorber for the 14.4 keV transition of ^{57}Fe; using this unit, we get $\beta_N = 0.6555$ (mm/s T). The nuclear g values g_I for the ground and the excited state of ^{57}Fe are $g_{1/2} = 0.18048$ and $g_{3/2} = -0.103$ [6]. The quantity g is the g-tensor of the electronic cluster wave function. The effective spin operator $\boldsymbol{S}_{eff}$ and the first

* We refer to reference [7] for definitions of tensor operators and their application in quantum mechanics.

rank tensor $\mathcal{T}^{(1)}$ operate on the electronic part of the system. $\boldsymbol{S}_{\text{eff}}$ operates on the center of the cluster wave function. Thus the cubic symmetry T_d has to be taken into account here. On the other hand $\mathcal{T}^{(1)}$ is connected with the hyperfine interaction of the cluster orbital wave function and the nuclear dipole moment of one individual iron nucleus. The appropriate point symmetry of this interaction is C_{3v} according to the trigonal symmetry of the iron site. $\mathcal{K}^{(1)}$ acts on the nuclear wave function. The nuclear matrix element to be evaluated is [7]

$$\langle I, m \,|\, \mathcal{K}_q^{(1)} \,|\, I, m' \rangle = (-1)^{I-m} \begin{pmatrix} I & 1 & I \\ -m & q & m' \end{pmatrix} \cdot \sqrt{I(I+1)\,(2I+1)}\,. \qquad (2)$$

Finally, the quadrupole coupling constant P_{zz} is given by $e\,Q(1-R)\cdot V_{zz}/4\,I(2\,I-1)$, where the threefold symmetry axis of an iron atom along the diagonal of the cube is chosen to be the z-axis.

Oxidized Ferredoxin

Because ferredoxin shows no ESR signal in the oxidized state [2], the eigenfunctions ψ_ν of the distorted cube are singlets, indicating that each Fd_{ox} cluster contains an even number of electrons. In this case only the last two terms of the Hamiltonian (1) contribute to the hyperfine spectrum of the iron atoms, because the non-degenerate eigenfunctions ψ_ν of the cluster are invariant unter time reversal. Accordingly, the relevant matrix elements $\langle \psi_\nu | \boldsymbol{S}_{\text{eff}} | \psi_\nu \rangle$ and $\langle \psi_\nu | \mathcal{T}^{(1)} | \psi_\nu \rangle$ vanish. It is worthwhile to note that the invariance under time reversal would be violated by an external magnetic field in the second-order approximation. However, the interaction energy $g\,\beta_0\,H_{\text{ext}}$ ($\approx 10\,\text{cm}^{-1}$ for $H_{\text{ext}} = 10\,\text{T}$) is certainly small when compared to the excitation energy of the cluster electrons. Thus no serious admixture of excited cluster states should take place which could affect the present calculations. In the absence of an external magnetic field only the third term of (1) exists and the Mössbauer spectrum consists of a quadrupole doublet with $1/2\,e^2\,q\,Q = 6\,P_{zz}$. The slight broadening and asymmetry of the lines found experimentally [2] indicate that the four iron atoms of the cluster are not exactly equivalent. This inequivalence, however, is neglected in our present calculations. A temperature dependence of $1/2\,e^2\,q\,Q$ is explainable by the thermal population of excited states of the cluster electrons. The total Hamiltonian of Fd_{ox} depends on the direction of $\boldsymbol{H}_{\text{ext}}$ relative to the trigonal axis (z-axis) at any particular iron site. In spherical polar co-ordinates the components of $\boldsymbol{H}_{\text{ext}}$ will be H_{ext} $(\sin\vartheta\cos\varphi,\ \sin\vartheta\sin\varphi,\ \cos\vartheta)$, where ϑ is the angle between the magnetic field and the z-axis. Because of the trigonal symmetry of the problem, the Hamiltonian depends on φ only in form of a phase factor which does not affect the calculations. Setting φ equal zero, the Hamiltonian of Fd_{ox} may be written

$$\mathcal{H}_{ox} = P_{zz}[3\,\mathcal{I}_z^2 - I(I+1)] - \beta_N\,g_I\,H_{\text{ext}}[\mathcal{I}_z\cos\vartheta + \tfrac{1}{2}(\mathcal{I}_+ + \mathcal{I}_-)\sin\vartheta]\,; \qquad (3)$$

the symbols $\mathcal{I}_\pm$ stand for $\mathcal{I}_x \pm \mathcal{I}_y$, respectively. Diagonalizing this Hamiltonian, we find the eigenvalues and eigenvectors for the ground state ($I = 1/2$) and for the 14.4 keV niveau ($I = 3/2$) of ^{57}Fe: 14.4 keV level ($I = 3/2$):

$$E_\mu\ (\mu = 1, \ldots, 4) \qquad (4\,a)$$
$$\psi_\mu = a_{\mu 1}\,|\tfrac{3}{2}\rangle + a_{\mu 2}\,|\tfrac{1}{2}\rangle + a_{\mu 3}\,|-\tfrac{1}{2}\rangle + a_{\mu 4}\,|-\tfrac{3}{2}\rangle$$

ground state ($I = 1/2$):

$$E_\nu^{(0)}\ (\nu = 1, 2)$$
$$\psi_\nu^{(0)} = b_{\nu 1}\,|\tfrac{1}{2}\rangle + b_{\nu 2}\,|-\tfrac{1}{2}\rangle \qquad (4\,b)$$

where the energies E_μ, $E_\nu^{(0)}$ and the coefficients $a_{\mu\lambda}$, $b_{\nu\varrho}$ are functions of the angle ϑ. We start the calculations using a fixed angle ϑ. The energies of the eight hyperfine lines, neglecting the trivial isomer shift are then

$$E_{\mu\nu} = E_\mu - E_\nu^{(0)}. \qquad (5)$$

The intensities of these lines depend on the multipolarity (the 14.4 keV transition of ^{57}Fe is almost a pure Ml radiation), the polarization and the direction $\boldsymbol{k}$ of the γ-ray. According to Frauenfelder *et al.* [8], we get the required transition amplitude for Ml radiation from the matrix elements

$$\langle I = \tfrac{3}{2}, m \,|\, A_\sigma \,|\, I_i = \tfrac{1}{2}, m_i \rangle = (-1)^{1/2 + m_i} \cdot \begin{pmatrix} 3/2 & 1 & 1/2 \\ m & M & -m_i \end{pmatrix} D^{(1)*}_{M\sigma}\ (z \rightarrow \boldsymbol{k}). \qquad (6)$$

Here, $D^{(1)}_{M\sigma} \equiv \langle M \,|\, D^{(1)} \,|\, \sigma \rangle$ are the elements of the rotation matrix; the argument $(z \rightarrow \boldsymbol{k})$ of the rotation matrix stands for the Euler angles (α, β, γ) describing the rotation that carries the quantization system z over into the co-ordinate system of the radiation, where $\beta = 0$. The index $\sigma = +1$ indicates right circular polarization, $\sigma = -1$ left circular

polarization. The relative intensities $I_{\mu\nu}$ of the hf-lines $E_{\mu\nu}$ for unpolarized radiation are defined by

$$I_{\mu\nu} = \sum_{\sigma=\pm 1} |\langle \psi_\mu | A_\sigma | \psi_\nu^{(0)} \rangle|^2 . \tag{7}$$

From Eqns (4) and (6) we obtain the following result

$$\begin{aligned} I_{\mu\nu} = {} & \tfrac{2}{3}(A_{\mu\nu}^2 + B_{\mu\nu}^2 + C_{\mu\nu}^2) \\ & + \tfrac{1}{6}(A_{\mu\nu}^2 - 2B_{\mu\nu}^2 + C_{\mu\nu}^2)(3\cos^2\beta - 1) \\ & + \sqrt{2}\, B_{\mu\nu}(A_{\mu\nu} - C_{\mu\nu}) \sin\beta\cos\beta\cos\alpha \\ & + A_{\mu\nu} C_{\mu\nu} \sin^2\beta \cos 2\alpha . \end{aligned} \tag{8}$$

The coefficients $A_{\mu\nu}$, $B_{\mu\nu}$ and $C_{\mu\nu}$, still depending on the angle ϑ, are given by

$$\begin{aligned} A_{\mu\nu} &= \tfrac{1}{2} a_{\mu 1} b_{\nu 1} + \frac{1}{2\sqrt{3}} a_{\mu 2} b_{\nu 2} , \\ B_{\mu\nu} &= \frac{1}{\sqrt{6}} (a_{\mu 2} b_{\nu 1} + a_{\mu 3} b_{\nu 2}) , \\ C_{\mu\nu} &= \tfrac{1}{2} a_{\mu 4} b_{\nu 2} + \frac{1}{2\sqrt{3}} a_{\mu 3} b_{\nu 1} . \end{aligned} \tag{9}$$

Setting $\beta = \vartheta$ and $\alpha = 0$, Eqn (8) defines the intensity of the hf-spectrum for a magnetic field applied parallel to the γ-ray direction. The Mössbauer spectrum for an iron atom situated on a site having an angle ϑ between its z-axis and $\boldsymbol{H}_{\text{ext}}$ can be simulated by a sum of Lorentzian lines according to the allowed hyperfine transitions. These lines are characterized by the same linewidth Γ_{exp} which is a variable parameter and has to be adjusted to the experimental spectrum. The lines are centered at $E_{\mu\nu}(\vartheta)$ as calculated from Eqns (4) and (5) and have an area proportional to $I_{\mu\nu}(\vartheta)$ as defined by Eqns (8) and (9). Iron sites with different angles ϑ are present even in one molecule. Thus iron sites having angles ϑ between 0 and π will simultaneously be present in a polycrystalline sample. In order to simulate the spectrum for a sample with randomly oriented molecules one has to sum up the spectra of the various iron sites with different angle ϑ weighted by the statistical factor $\sin\vartheta$.

Although it might at first sight appear natural to define the quantization axis z in Eqn (3) along the trigonal axis of the iron sites *, this would lead to problems in the evaluation of the intensities $I_{\mu\nu}$ for γ-ray directions not parallel to the applied magnetic field. In addition it becomes difficult to take into account the angular divergence of the γ-beam. The suitable quantization axis to be chosen for our numerical calculations is an axis parallel to the applied magnetic field. The appropriate transformation of the Hamiltonian (3) into this co-ordinate system is given in the Appendix. The problem of divergence of the beam of the γ-ray is also discussed there.

Figure 2 shows the Mössbauer spectra of Fd_{ox} in an external magnetic field of 6 T calculated along the lines just described. The direction of the γ-ray is *perpendicular* to the field $\boldsymbol{H}_{\text{ext}}$ and an angular divergence of $\varepsilon = 8^\circ$ has been assumed (see Appendix equation (A 10)). A broadening of the emission line due to magnetic stray-fields at the source position has not explicitly been taken into account. An effective linewidth of 0.45 mm/s was chosen which may involve the stray-field effect and the effect of the slight inequivalence of the iron sites. The value P_{zz} is taken from the mean quadrupole splitting $|1/2\, e^2 q Q| = 1.1$ mm/s found at 4.2 K and $\boldsymbol{H}_{\text{ext}} = 0$ [2, 3]. The difference in the two spectra of Fig. 2 arises from the choice of the sign of the quadrupole interaction which cannot be determined from the experiments at $\boldsymbol{H}_{\text{ext}} = 0$. Fig. 2 a shows a better agreement with the experimental result, published in Fig. 1 of reference [3]. This indicates a positive electric field gradient since for the 14.4 keV state of ^{57}Fe Q equals $+0.19$ b.

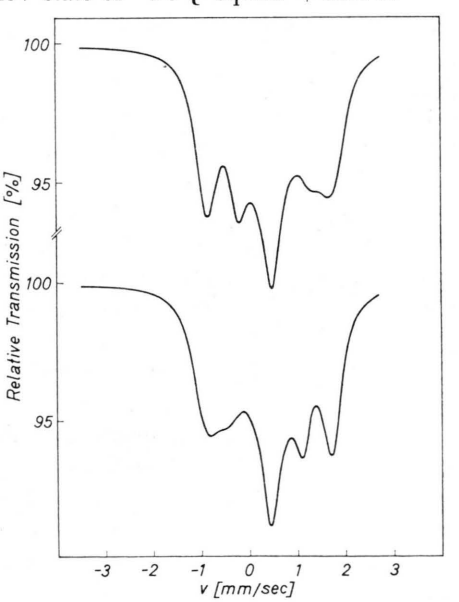

Fig. 2. Calculated Mössbauer spectra of Fd_{ox} at 4.2 K for an external applied magnetic field of $H_{\text{ext}} = 6$ T. a. $q > 0$; b. $q < 0$. $\boldsymbol{k}$ (γ) $\perp \boldsymbol{H}_{\text{ext}}$.

* More generally, the z-axis in Eqn (3) defines that direction in which the asymmetry parameter η of the quadrupole interaction becomes a minimum.

Mössbauer spectra of model compounds forming (iron)$_4$-sulfur clusters have been published [9–11]. Using the parameters given in the caption to Fig. 1 of reference [11] in our calculations yields a spectrum which is in agreement with the experimental data and the spectrum simulation published in reference [11]. Also in this case a positive electric field gradient is found.

Reduced Ferredoxin

ESR-data [2] indicate that on reduction each (iron)$_4$-sulfur cluster of the ferredoxin gains one electron. The resulting odd number of electrons in each cluster together with the invariance under time reversal imply a twofold degeneracy of all unperturbed cluster eigenfunctions (Kramers-degeneracy). Therefore, an isolated cluster is expected to show magnetic spectra even in the absence of an external magnetic field at least at low temperatures. These have been found in the case of the oxidized Chromatium high-potential iron-sulfur protein where each molecule contains one (iron)$_4$-sulfur cluster with an odd number of electrons [12]. The *Clostridium pasteurianum* ferredoxin, however, contains two (iron)$_4$-sulfur clusters per molecule which interact weakly via spin-spin coupling and the overlap of the cluster orbitals in the reduced state [2]. The structural unit for the wave function is then the two-cluster system, rather than the isolated cluster. The representation of the total wave functions being still invariant under time reversal is thus the direct product of the two valued representations of the isolated clusters (Kramers-doublets). This then gives rise to non-degenerate eigenfunctions as in the case of oxidized ferredoxin. The necessary dominance of the cluster-cluster interaction over the small magnetic hyperfine interaction ($\lesssim 10^{-3}\,\mathrm{cm}^{-1}$) is proven experimentally in reference [2, 3] since no magnetic hyperfine spectrum could be observed in the absence of an applied field even at lowest temperatures.

The invariance under time reversal is lifted in the presence of an external magnetic field provided that its interaction with the cluster wave function (first term of Eqn (1)) is significantly greater than the cluster-cluster interaction. Throughout the remainder of the paper we assume that the applied magnetic field is larger than 1 T which should render the cluster-cluster interaction to be negligible. The wave function of the basic Kramers-doublet of each cluster can then be written in the form

$$\psi_0 = C_1 |+\rangle + C_2 |-\rangle . \tag{10}$$

By making use of the (nearly) trigonal point symmetry of an iron site, the required matrix elements of the magnetic hyperfine interaction as given by Eqn (1) can be related to two real parameters $\varkappa$ and ϱ which finally have to be adjusted to the experimental data.

$$\begin{aligned} \langle \pm | \mathcal{T}_0^{(1)} | \pm \rangle &= \pm \varkappa \\ \langle + | \mathcal{T}_1^{(1)} | - \rangle &= \varrho \\ \langle - | \mathcal{T}_{-1}^{(1)} | + \rangle &= -\varrho \end{aligned} \tag{11}$$

The deviation from C_{3v} symmetry which is neglected here would lead to a complex parameter ϱ. The first term of Eqn (1) defines the Zeeman splitting of the Kramers-doublet by an applied magnetic field. Because of the nearly cubic symmetry of a cluster, the average g-tensor is assumed to be isotropic in agreement with ESR data ($g = 1.944$) *. If the quantization axis is directed along the trigonal axis, then the components of the applied field (setting $\varphi = 0$) become again $\boldsymbol{H}_{\mathrm{ext}} = H_{\mathrm{ext}}(\sin\vartheta, 0, \cos\vartheta)$. Under the action of the Zeeman term in Eqn (1), we get the following eigenvalues and eigenvectors of the split Kramers-doublet:

$$\begin{aligned} E_1 &= -\tfrac{1}{2}\beta_0 g H_{\mathrm{ext}} \\ |1\rangle &= \sin(\vartheta/2)|+\rangle - \cos(\vartheta/2)|-\rangle \\ E_2 &= +\tfrac{1}{2}\beta_0 g H_{\mathrm{ext}} \\ |2\rangle &= \cos(\vartheta/2)|+\rangle + \sin(\vartheta/2)|-\rangle . \end{aligned} \tag{12}$$

At low temperatures ($T = 4.2$ K) the spin-lattice relaxation time becomes long compared to the precession time of the magnetic dipole moment of the ^{57}Fe nuclei. Each Zeeman-level generates then a separate hf-spectrum. Eqn (1) shows that the quadrupole coupling and the direct interaction of the applied field with the nucleus are identical for both these spectra, while this is not true for the magnetic dipole interaction. In fact, one gets from Eqns (11) and (12)

$$\begin{aligned} \langle 1 | \mathcal{T}_0^{(1)} | 1 \rangle &= -\langle 2 | \mathcal{T}_0^{(1)} | 2 \rangle = -\varkappa\cos\vartheta \\ \langle 1 | \mathcal{T}_1^{(1)} | 1 \rangle &= -\langle 2 | \mathcal{T}_1^{(1)} | 2 \rangle = -\tfrac{1}{2}\varrho\sin\vartheta \\ \langle 1 | \mathcal{T}_{-1}^{(1)} | 1 \rangle &= -\langle 2 | \mathcal{T}_{-1}^{(1)} | 2 \rangle = +\tfrac{1}{2}\varrho\sin\vartheta . \end{aligned} \tag{13}$$

* ESR measurements on *Clostridium pasteurianum* ferredoxin reduced only in one cluster led to $g_{zz} = 2.05$ and $g_{xx} = g_{yy} = 1.92$ [2].

The nuclear matrix elements needed for the evaluation are given in Eqn (2). The energies and intensities of the hf-spectrum of Fd_{red} can now be calculated from the modified Hamiltonian along the lines described for oxidized ferredoxin. It should be pointed out that the intensities of the two "Zeeman-level" hf-spectra being superimposed in the experimental Mössbauer spectrum must be weighted by the appropriate Boltzmann factor which is obtained from the Zeeman splitting energies in Eqn (12). Thus, one expects a temperature dependence of the magnetic dipole interaction according to the changing population of the two Zeeman-levels.

Using this theory, we have performed least squares fit procedure to the experimental Mössbauer spectrum. A theoretical spectrum was first calculated as a function of four independent parameters. They were in addition to ϱ and $\varkappa$ the theoretical value of the counting rate at $v=\infty$ and a normalization factor for the overall absorption depth. This factor includes the f-factors of the source and the absorber, the thickness of the absorber and the non-resonant background in the gamma energy window around 14.4 keV. These four parameters were varied until a theoretical spectrum could be obtained which, according to least squares fit criteria, gave the best agreement with the experimental data. As fixed parameter we used in the calculation the quadrupole interaction of $|1/2\, e^2 q Q| = 1.54$ mm/s derived from spectra at 4.2 K without an external magnetic field [1-3]. Again, both a positive and a negative electric field gradient have been assumed in separate fits. Another fixed parameter is the effective width Γ_{eff} of the Lorentzian resonance lines which again includes inherently the line broadenings brought about from the magnetic stray-field acting on the source and from the slight inequivalence of the quadrupole interaction at the various iron sites. In our experiments a source of ^{57}Co in Rh has been used which gives only a moderate line broadening at $H_{\text{ext}}=2$ T, although the source was directly mounted on top of the absorber. In the fits a uniform value of $\Gamma_{\text{eff}}=1.1$ mm/s has been used. Strictly speaking, one has to take into account also polarization effects arising from the external magnetic field acting both on source and absorber [14]. We estimate the resulting line distortion to be negligible in first order in connection with the Co(Rh) source and the moderately low field used in the experiment.

In order to reduce the computer time needed for the calculation of each theoretical spectrum in the least squares procedure the following simplification has been used. For any single set of parameters we first calculated the transition energies $E_{\mu\nu}$ for a specific angle ϑ. The total energy scale of the Mössbauer spectrum ranging ± 25 mm/s was subsequently divided into energy channels of constant width of 0.05 mm/s. The intensities $I_{\mu\nu}(\vartheta)$ were then assigned to the corresponding channels. This procedure is then repeated for the next angle ϑ in steps of $\Delta\vartheta=2^\circ$ between $\vartheta=0$ and $\vartheta=\pi$. The summation of the intensities $I_{\mu\nu}(\vartheta)$ with the appropriate statistical weight yields the total intensities I_i for the different channels. Normalization then gives

$$I_i' = I_i / \sum_i I_i . \tag{14}$$

Intensities below a certain value $I'_{\min}=0.001$ are set identical to zero. The next step is then to center at each channel a Lorentzian with a half width of Γ_{eff} and an intensity of I'_i. The summation of these Lorentzians along the lines explained above for the case of Fd_{ox} then gives the theoretical spectrum for any set of variable parameters.

In Fig. 3 such least squares fits to the Mössbauer spectrum of Fd_{red} measured at 4.2 K and in an external field of $H_{\text{ext}}=2$ T parallel to the direction of γ-ray propagation are shown. Both, a positive (Fig. 3 a) and a negative electric field gradient q have been assumed. Again $q>0$ gives a sightly more favourable fit, although in neither case the agreement is perfect due to the simplifications outlined above. The fit of Fig. 3 a yields the following values for the magnetic hyperfine parameters:

$$\varkappa = -6.5\ \text{T}$$
$$\text{and} \quad \varrho = 12.1\ \text{T}\ ^*. \tag{15}$$

In order to discuss the physical significance of these parameters we remind ourselves that the hyperfine interaction at the iron nuclei can be interpreted as arising from the sum of two effective but not parallel magnetic fields generated by the Zeeman levels of the Fd_{red} groundstate. Each effective interaction may be written as:

$$\mathcal{H}_m = \beta_N g_I \langle n | \boldsymbol{H}_{\text{eff}} | n \rangle \cdot \boldsymbol{I} \tag{16}$$

where n refers to the two Zeeman levels. From the definition of the magnetic hf-interaction in Eqn (1)

* Fig. 3 b ($q<0$) yields $\varkappa=-9.2$ T and $\varrho=10.6$ T.

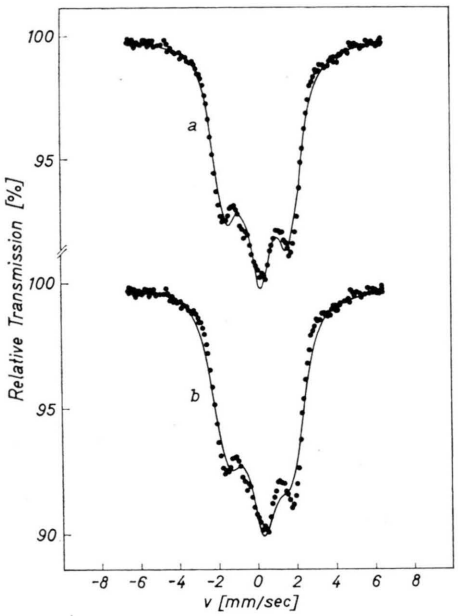

Fig. 3. Least squares fits of the Mössbauer spectrum of Fd_{red} at 4.2 K for an external applied magnetic field of $H_{ext}=2$ T. a. $q>0$; b. $q<5$. $\boldsymbol{k}$ $(\gamma) \parallel \boldsymbol{H}_{ext}$.

we find from Eqn (13)

$$\langle 1 | H_{eff}^{\parallel} | 1 \rangle = -\langle 2 | H_{eff}^{\parallel} | 2 \rangle = -\varkappa \cos\vartheta \quad (17)$$

$$\langle 1 | H_{eff}^{\perp} | 1 \rangle = -\langle 2 | H_{eff}^{\perp} | 2 \rangle = +\frac{1}{\sqrt{2}} \varrho \sin\vartheta$$

where H_{eff} and $H_{eff}^{\perp}$ can then be interpreted as the components of a magnetic hyperfine field directed parallel and perpendicular to the trigonal axis of an iron site. If one considers only the four neighboring sulfur atoms (see Fig. 1), the iron sites in each cluster would have tetrahedral point symmetry. In this isotropic case the relation $\varrho = -\sqrt{2}\varkappa$ would hold and the two magnetic hyperfine fields are parallel, respectively antiparallel to the applied field direction. The values of $\varkappa$ and ϱ as returned from the fit, however, show that the isotropic case is not a good approximation and that the lower trigonal point symmetry for the iron sites has definitely to be taken into account.

Fig. 4 shows a least squares fit to the spectrum of Fd_{red} measured at 4.2 K with $H_{ext}=1$ T parallel to the γ-ray. The fit for $q>0$ yields $\varkappa=-6.6$ T and $\varrho=10.4$ T. The choice of a negative electric field gradient produces an equally acceptable fit.

The theoretical spectra of Fig. 4 reproduce the resonance lines fairly well, their intensities, however, are only in rather crude agreement. The values

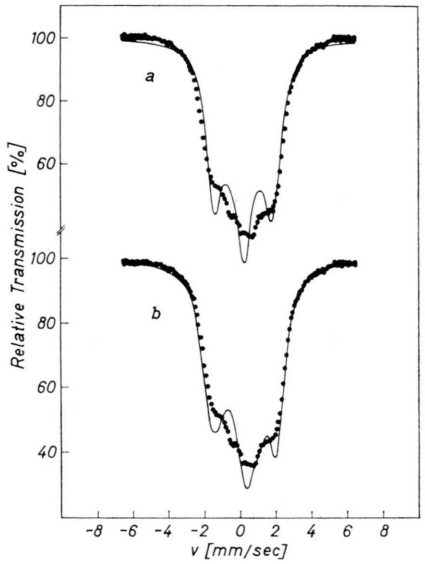

Fig. 4. Least squares fits of the Mössbauer spectrum of Fd_{red} at 4.2 K for an external applied magnetic field of $H_{ext}=1$ T. a. $q>0$; b. $q<0$.

for the magnetic parameters $\varkappa$ and ϱ quoted above are roughly the same as in the case of the 2 T spectrum. This proves our original assumption that each cluster interacts independently with H_{ext} for $H_{ext} \geqq 1$ T. The energy separation of the two Zeeman levels will be proportional to H_{ext}. A relaxation process between these levels then has to depend strongly on the size of H_{ext}. The fact that the values of the parameters $\varkappa$ and ϱ do not change significantly between $1\,\mathrm{T} \leqq H_{ext} \leqq 2\,\mathrm{T}$ indicates, that such relaxation processes are not significant at temperatures as low as 4.2 K. Finally, using the formalism of transformation of quantization axes given in the Appendix we have simulated some Mössbauer spectra of Fd_{red} at 4.2 K with the external magnetic field acting perpendicular to the direction of the γ-ray beam. The magnetic parameters ϱ and $\varkappa$ were fixed to the values returned by the fit shown in Fig. 3 a. Data for Fd_{red} in a perpendicular-external field have been reported by Thompson *et al.*[3]. A comparison with their data shows, that our calculated spectra cover the same velocity range but have a considerably better resolved structure. This discrepancy exists over the whole range of external field strength up to 6 T. It can easily arise from the before-mentioned neglect of the slight site difference of the four cluster irons which lifts their C_{3v} point symmetry. As discussed above, such a perturbation of trigonal symmetry implies that ϱ

becomes a complex number, thus increasing the number of magnetic fit parameters to three. In addition one has then to perform the angular average not only with respect to ϑ but also for the angle φ. This means a considerable increase in computational time and thus has not been carried out.

Concluding Remarks

The theory and fitting procedure described thus far gives results in reasonable agreement with the experimental data on Fd_{ox} and Fd_{red}. In particular it could be shown that the magnetic interactions are consistent with both the known structural arrangement of the iron atoms in the cluster and the assumption of highly delocalized electrons which have to be described by cluster orbital wave functions. Some improvements on the present calculating routine can be made and are presently being carried out. Instead of the sum of Lorentzians used to generate the theoretical spectra it is more favorable to employ a procedure based on the full transmission integral [13]. Such a calculation is a marked improvement especially for the determination of the intensities of closely overlapping resonance lines. In addition this program lends itself to an inclusion of the already mentioned polarization effects arising from the action of the external magnetic field on the source nuclei. This correction is important for high field measurements which show considerably more detailed structure (see for example Fig. 4 of reference [3]). Along this line new experiments are being performed using a very strong ^{57}Co in Rh source situated further away from the field generated by the superconducting solenoid.

This work was supported by the Deutsche Forschungsgemeinschaft. We are indebted to Prof. Dr. G. M. Kalvius for his continuous support of our work.

Appendix

In this appendix it is shown how the hyperfine interaction Hamiltonian of Eqn (1) is transformed to a co-ordinate system in which the quantization axis is directed along the direction of the applied magnetic field. In addition the results obtained by this transformation are put into a form more suitable for numerical computations.

The generalized quadrupole interaction is described by the Hamiltonian [7]

$$\mathcal{H}_Q = \sum_q (-1)^q \mathcal{V}_q^{(2)} \mathcal{K}_{-q}^{(2)} \qquad \text{(A 1)}$$

where $\mathcal{V}_q^{(2)}$ is proportional to the electric field gradient tensor and $\mathcal{K}^{(2)}$ is a tensor of rank 2 acting on the nuclear wave function; its relevant matrix elements are given by

$$\langle I, m \,|\, \mathcal{K}_q^{(2)} \,|\, I, m' \rangle = 6\sqrt{5}(-1)^{I-m} \begin{pmatrix} I & 2 & I \\ -m & q & m' \end{pmatrix} \qquad \text{(A 2)}$$

Setting

$$\mathcal{V}_q^{(2)} = P_{zz}\, \delta_{q,0} \qquad \text{(A 3)}$$

the Hamiltonian $\mathcal{H}_Q$ is identical with the quadrupole term of Eqn (1). The transformation of the tensor $\mathcal{V}^{(2)}$ to the new co-ordinate system is carried out by application of the rotation matrix $D^{(2)}(z \rightarrow z')$:

$$\mathcal{V}_q^{(2)\prime} = \sum_\mu D_{q\mu}^{(2)}\,(0, \vartheta, 0)\, \mathcal{V}_\mu^{(2)}. \qquad \text{(A 4)}$$

The magnetic dipole interaction in Eqn (1) involves the first-rank tensor $\mathcal{T}^{(1)}$ representing the interaction of the two Zeeman levels (12) of the Fd_{red} cluster with the magnetic dipole moment of the ^{57}Fe nucleus; components of $\mathcal{T}^{(1)}$ for the two Zeeman levels, respectively, are given in Eqn (13). In analogy to Eqn (A 4) the transformation of the tensor $\mathcal{T}^{(1)}$ is then carried out by the equation

$$\mathcal{T}_q^{(1)\prime} = \sum_\mu D_{q\mu}^{(1)}\,(0, \vartheta, 0)\, \mathcal{T}_\mu^{(1)}. \qquad \text{(A 5)}$$

The transformed hf-Hamiltonian of Eqn (1) becomes finally

$$\mathcal{H}'_{hf} = \beta_N g_I \sum_q (-1)^q \mathcal{T}_q^{(1)\prime} \mathcal{K}_{-q}^{(1)} + \sum_q (-1)^q \mathcal{V}_q^{(2)\prime} \mathcal{K}_{-q}^{(2)} - \beta_N g_I H_{ext} I_z \qquad \text{(A 6)}$$

where the components of $\mathcal{V}^{(2)\prime}$ and $\mathcal{T}^{(1)\prime}$ written in detail are

$$\begin{aligned} \mathcal{V}_0^{(2)\prime} &= P_{zz}\, \tfrac{1}{2}(3\cos^2\vartheta - 1) \\ \mathcal{V}_{\pm 1}^{(2)\prime} &= \pm P_{zz}\sqrt{3/2}\cos\vartheta \sin\vartheta \\ \mathcal{V}_{\pm 2}^{(2)\prime} &= P_{zz}\sqrt{3/8}\sin^2\vartheta \end{aligned} \qquad \text{(A 7)}$$

and

$$\begin{aligned} \langle 1 \,|\, \mathcal{T}_0^{(1)\prime} \,|\, 1 \rangle &= -\langle 2 \,|\, \mathcal{T}_0^{(1)\prime} \,|\, 2 \rangle \\ &= \frac{\varrho}{\sqrt{2}}\sin^2\vartheta - \varkappa\cos^2\vartheta \\ \langle 1 \,|\, \mathcal{T}_{\pm 1}^{(1)\prime} \,|\, 1 \rangle &= -\langle 2 \,|\, \mathcal{T}_{\pm 1}^{(1)\prime} \,|\, 2 \rangle \\ &= \mp\left(\frac{\varrho}{4} + \frac{\varkappa}{2\sqrt{2}}\right)\sin 2\vartheta\,. \end{aligned} \qquad \text{(A 8)}$$

The intensities $I_{\mu\nu}$ of the hf-lines can directly be computed from the general formula (8). However, the coefficients $A_{\mu\nu}$, $B_{\mu\nu}$, $C_{\mu\nu}$ are to be obtained by the modified Hamiltonian (A 6) and β is now the angle between the γ-ray and the direction of the applied magnetic field. No physical significance is attached to the angle α for unpolarized radiation; one therefore averages the intensity $I_{\mu\nu}$ with respect to α and has:

$$\langle I_{\mu\nu} \rangle_\alpha = 1/2\,\pi \int_0^{2\pi} I_{\mu\nu}\,\mathrm{d}\alpha\,. \qquad \text{(A 9)}$$

This leads to

$$I_{\mu\nu} = \tfrac{2}{3}\,(A_{\mu\nu}^2 + B_{\mu\nu}^2 + C_{\mu\nu}^2) + \tfrac{1}{6}\,(A_{\mu\nu}^2 - 2\,B_{\mu\nu}^2 + C_{\mu\nu}^2)\,(3\cos^2\beta - 1)\,. \qquad \text{(A 10)}$$

The finite size of the γ-ray detector causes an angular spread ε around the angle β.

Hence the value of $(3\cos^2\beta - 1)$ must be corrected for such a spread. The proper averaging gives

$$\langle 3\cos^2\beta - 1 \rangle_\varepsilon = \frac{2}{\varepsilon^2} \int_0^{\varepsilon} \Theta\,[3\cos^2(\beta + \Theta) - 1]\,\mathrm{d}\Theta$$

$$= (3\cos^2\beta - 1) - 2\,\varepsilon \sin 2\beta - \tfrac{3}{2}\varepsilon^2 \cos 2\beta\,. \qquad \text{(A 11)}$$

which then is to be inserted into Eqn (A 10).

[1] F. Parak, W. Zgorzalla, H. Eicher, G. M. Kalvius, K. Gersonde, M. Breitenbach, H. E. Schlaak, and A. Mayer, Proceedings of The 5th International Conference on Mössbauer Spectrometry, Bratislava, Czechoslovakia, Sept. 3—7, 1973, to be published.

[2] K. Gersonde, H. E. Schlaak, M. Breitenbach, F. Parak, H. Eicher, W. Zgorzalla, G. M. Kalvius, and A. Mayer, Eur. J. Biochem. **43**, 307—317 [1974].

[3] C. L. Thompson, C. E. Johnson, D. P. E. Dickson, R. Cammack, D. O. Hall, U. Weser, and K. K. Rao, Biochem. J. **139**, 97—103 [1974].

[4] L. C. Sieker, A. Adman, and L. H. Jensen, Nature **235**, 40—42 [1972].

[5] E. T. Adman, L. C. Sieker, and L. H. Jensen, J. Biol. Chem. **248**, 3987—3996 [1973].

[6] A. H. Muir, K. J. Ando, and H. M. Coogan, Mössbauer Effext Data Index, 1958—1965, Interscience Publishers, John Wiley and Sons, New York 1966. J. G. Stevens and V. E. Stevens, Mössbauer Effect Data Index covering the 1971 literature IFI/Plenum Press, New York 1972.

[7] B. R. Judd, Operator Techniques in Atomic Spectroscopy, Advanced Physics Monograph Series (W. A. Nierenberg, ed.), MacGraw-Hill Book, New York 1963.

[8] H. Frauenfelder, R. M. Steffen, S. R. De Groot, H. A. Tolhoek, and W. J. Huiskamp, Alpha, Beta and Gamma Ray Spectroscopy (E. Siegbahn, ed.), North Holland Publishing Company, Amsterdam 1965.

[9] R. H. Holm, B. A. Averill, T. Herskovitz, R. B. Frankel, H. B. Gray, O. Süman- and F. J. Grunthaner, Amer. Chem. Soc. **96**, 2644—2646 [1974].

[10] R. B. Frankel, T. Herskovitz, B. A. Averill, R. H. Holm, P. J. Krusic, and W. D. Phillips, Biochem. Biophys. Res. Commun. **58**, 974—982 [1974].

[11] R. B. Frankel, W. M. Reiff, I. Bernal, and M. L. Good, Inorg. Chem. **13**, 493—494 [1974].

[12] D. P. E. Dickson, C. E. Johnson, R. Cammack, M. C. W. Evans, D. O. Hall, and K. K. Rao, Biochem. J. **139**, 105—108 [1974].

[13] G. K. Shenoy, J. M. Friedt, H. Maletta, and S. L. Ruby, Mössbauer Effect Methodology, 1974 to be published.

[14] H. Maletta, R. B. Frankel, W. Hennin, and R. L. Mössbauer, Phys. Letters **28 A**, 557—558 [1969].